ACS APPLIED MATERIALS & INTERFACES

Research Article

www.acsami.org

An Anisotropically and Heterogeneously Aligned Patterned Electrospun Scaffold with Tailored Mechanical Property and Improved Bioactivity for Vascular Tissue Engineering

He Xu,[†,‡] Haiyan Li,[†] Qinfei Ke,[‡] and Jiang Chang*[,†,§]

[†]School of Biomedical Engineering and Med-X Research Institute, Shanghai Jiao Tong University, No.1954 Huashan Road, Shanghai 200030, China

[‡]College of Life and Environmental Sciences, Shanghai Normal University, No.100 Guilin Road, Shanghai 200234, China

[§]State Key Laboratory of High Performance Ceramics and Superfine Microstructure, Shanghai Institute of Ceramics, Chinese Academy of Sciences, No.1295 Dingxi Road, Shanghai 200050, China

ABSTRACT: The development of vascular scaffolds with controlled mechanical properties and stimulatory effects on biological activities of endothelial cells still remains a significant challenge to vascular tissue engineering. In this work, we reported an innovative approach to prepare a new type of vascular scaffolds with anisotropically and heterogeneously aligned patterns using electrospinning technique with unique wire spring templates, and further investigated the structural effects of the patterned electrospun scaffolds on mechanical properties and angiogenic differentiation of human umbilical vein endothelial cells (HUVECs). Results showed that anisotropically aligned patterned nanofibrous structure was obtained by depositing nanofibers on template in a structurally different manner, one part of nanofibers densely deposited on the embossments of wire spring and formed cylindrical-like structures in the transverse direction, while others loosely suspended and aligned along the longitudinal direction, forming a three-dimensional porous microstructure. We further found that such structures could efficiently control the mechanical properties of electrospun vascular scaffolds in both longitudinal and transverse directions by altering the interval distances between the embossments of patterned scaffolds. When HUVECs were cultured on scaffolds with different microstructures, the patterned scaffolds distinctively promoted adhesion of HUVECs at early stage and proliferation during the culture period. Most importantly, cells experienced a large shape change associated with cell cytoskeleton and nuclei remodeling, leading to a stimulatory effect on angiogenesis differentiation of HUVECs by the patterned microstructures of electrospun scaffolds, and the scaffolds with larger distances of intervals showed a higher stimulatory effect. These results suggest that electrospun scaffolds with the anisotropically and heterogeneously aligned patterns, which could efficiently control the mechanical properties and bioactivities of the scaffolds, might have great potential in vascular tissue engineering application.

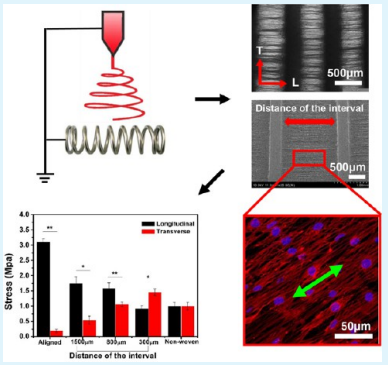

KEYWORDS: *electrospinning, pattern, mechanical property, bioactivity, vascular tissue engineering*

1. INTRODUCTION

Nowadays, cardiovascular disease is regarded as the leading cause of morbidity and mortality worldwide, and the strong demand for cardiovascular grafts has constantly been increasing, while key challenges associated with the outcome of vascular grafting remain unsolved.[1−3] The emerging vascular tissue engineering scaffolds offer an attractive "off-the-shelf" alternative as such scaffolds can be predesigned and prepared to address the specific need in clinical applications.[4−6] An ideal vascular scaffold should mimic not only the organized structure but also the physiological function of a normal blood vessel, which is crucial to successful vascular tissue engineering.

Many fabrication approaches have been explored with the aim to produce such an appropriate vascular tissue engineering scaffold, such as self-assembly, phase inversion, foaming procedures, particle leaching, and so on.[7,8] Among them, electrospinning, as a simple yet versatile manufacturing method to process a rich variety of biomaterials into nanofibers, has recently been garnering a lot of attention as the scaffolds obtained through electrospinning possess many attractive features, such as high surface area to volume ratio, formation of interconnected porous networks, similarity in fiber size scale to those of the extra cellular matrix (ECM) of native vasculature, and adjustable surface structure. These advantages make the electrospun nanofibrous scaffolds a favorable candidate for vascular tissue engineering.[9−11]

However, there are still two significant challenges for electrospun vascular scaffolds. First, it has been already known that a vascular scaffold should be able to resist the shear force exerted by blood flow along the longitudinal

Received: February 2, 2015
Accepted: March 31, 2015
Published: March 31, 2015

DOI: 10.1021/acsami.5b00996
ACS Appl. Mater. Interfaces 2015, 7, 8706−8718

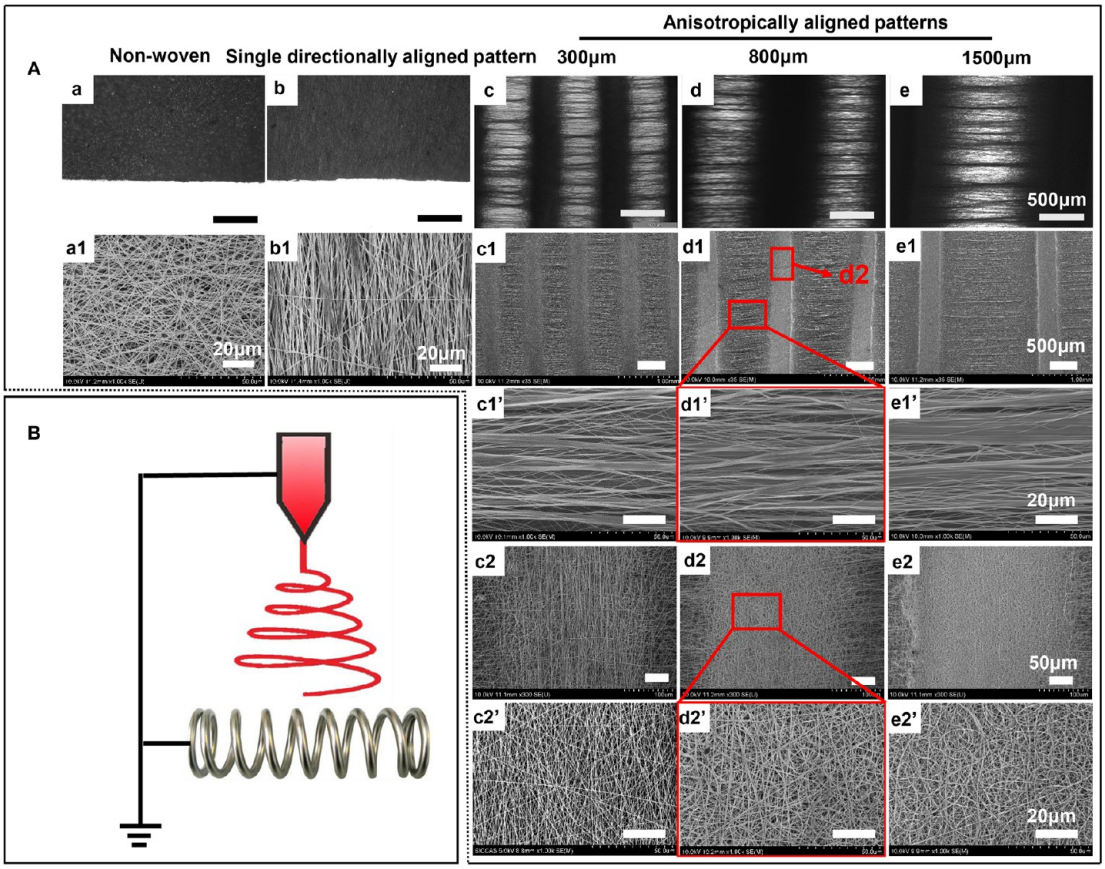

Figure 1. (A) Electrospun scaffolds with various structures prepared with different collecting devices. Optical images (a−e) and SEM images (a1−e1) in (A) show the electrospun scaffolds with different aligned patterns: (a,a1) nonwoven; (b,b1) single directionally aligned pattern; anisotropically aligned patterns with distances of intervals were 300 (c,c1), 800 (d,d1), and 1500 μm (e,e1), respectively. The high-magnification SEM images of the aligned nanofibers between the embossments in c1−e1 are shown in c1′−e1′, and the higher magnification images of nanofibers deposited on the embossments in c1−e1 are shown in c2−e2 (higher magnification) and c2′−e2′ (the highest magnification), respectively. (B) Schematic illustration of the preparation of anisotropically aligned patterned electrospun scaffolds.

direction while maintaining structural integrity until mature tissue forms in vivo. Moreover, because the blood dashes against the vascular wall continuously, the radial mechanical strength of vascular scaffolds should be strong enough to withstand the pulsatile nature of blood flow as well. Therefore, the appropriate vascular scaffold should provide sufficient mechanical strengths not only in longitudinal directions but also radial directions. Undoubtedly, either the traditional electrospun scaffolds with randomly deposited electrospun nanofibers or electrospun scaffolds composed of single directionally aligned nanofibers cannot efficiently control the tensile strengths of scaffolds in both longitudinal and radial directions simultaneously,[12−14] especially for that in the radial direction, which is of great importance for meeting the mechanical requirements of ideal vascular scaffolds.[15,16] Second, the design and fabrication of vascular tissue engineering scaffolds with appropriate surface architectures to induce cell growth and angiogenesis represent another major challenge. A series of studies have well demonstrated that the appropriate surface topography of scaffolds could promote various cellular processes, including adhesion, proliferation, and migration.[17−20] Furthermore, the specific surface physical cues could even guide the direction of cell differentiation. Lei et al. have demonstrated that the narrow stripes on micropatterned surfaces may result in the organization of vascular endothelium cells into tubular structures and the induction of sprouting angiogenesis, which is of great importance to regenerate vascularized tissues.[21,22] However, the current tissue engineering scaffolds with randomly deposited or single directionally aligned nanofibers seem to be not able to provide enough and effective topographic cues to guide the cell behaviors. So far, little effort has been devoted to the fabrication of electrospun vascular scaffolds with well-defined structural patterns, and the structural effects of the patterned electrospun scaffolds on the vascular endothelial cell behavior are still unclear.[16,23]

To achieve an electrospun vascular scaffold with adjustable mechanical properties in both longitudinal and radial directions, we hereby design a unique electrospun nanofibrous vascular scaffold with anisotropically and heterogeneously aligned structure. By using wire spring as a template collector, we hypothesize that nanofibers will deposit in different regions of the collector in a structurally different manner due to the varied electrostatic force, and with the unique structure of the wire spring collector, electrospun vascular scaffolds with aligned nanofibrous structures in both longitudinal and radial directions may be obtained, and such structurally anisotropic scaffolds can not only withstand the forces along the radial directions of scaffolds, but also provide structural cues to stimulate angiogenesis of vascular endothelial cells.

On the other hand, in our previous study, we have proofed that the combination of D,L-poly(lactic acid) (PDLLA) and poly(ε-caprolactone) (PCL) has better pattern formation

DOI: 10.1021/acsami.5b00996
ACS Appl. Mater. Interfaces 2015, 7, 8706−8718

ability and mechanical stability in wet condition.[11] Therefore, PDLLA/PCL composite was selected, and gelatin was added into the composite to further improve the biocompatibility. In this work, PDLLA/PCL/gelatin electrospun scaffolds with anisotropically and heterogeneously aligned patterns were fabricated. Wire springs with different interval distances (300, 500, and 1500 μm) were applied as collector templates to obtain patterned scaffolds with different interval distances between two embossments, and then microstructures and mechanical properties of the scaffolds were systematically investigated. Finally, the structural effects of the electrospun scaffolds with anisotropically aligned patterns on morphology, proliferation, and differentiation of human umbilical vein endothelial cells (HUVECs) were studied, and the possible mechanism was proposed.

2. MATERIALS AND METHODS

2.1. Materials. Poly(D,L-lactide) (PDLLA, M_w = 45 kDa) was purchased from Jinan Daigang Biomaterial Co, Ltd. (Shandong, China). Polycaprolactone (PCL, M_w = 80 kDa) was purchased from Sigma Co. Analytical grade gelatin and hexafluoro-2-propanol (HFIP) (≥99.5%) were purchased from Sinopharm Chemical Reagent Co. (Shanghai, China).

2.2. Electrospinning Preparation of Scaffolds with Anisotropically Aligned Patterns. For the preparation of electrospun scaffolds with anisotropically aligned patterns, a special wire spring collector (as shown in Figure 1B) was applied in the electrospinning setup. In a typical experimental procedure, the blend of PDLLA, PCL, and gelatin with a certain mass ratio (w/w/w = 35/35/30) was dissolved in HFIP, and then stirred for 6 h to obtain a homogeneous and stable solution with polymer concentration of 4.8% (w/v). The flow rate of the solution in the syringe (2 mL) was 0.02 mL m^{-1} by using a syringe pump (LSP01-1A, Baoding Longer Precision Pump, China). The voltage applied to the needle of the syringe was 8 kV. The distance between the tip of the needle and the collector was 12 cm. In this process, the external diameter of the wire spring is 2 cm, and the wire diameter is 0.3 mm. The wire spring was placed horizontally on a conductive plate, and by applying certain pressure on both ends of the spring, the pitch of thread could be controlled to modulate the interval distance. After electrospun nanofibers were directly deposited on the surface of the spring, the patterned electrospun scaffolds with different interval distances (300, 800, and 1500 μm) were obtained. In addition, aligned nanofibrous scaffolds were fabricated by electrospinning process using a rotating drum collector (2500 r/min), and the nonwoven nanofibrous scaffolds were also prepared using a plane collector as controls. To obtain scaffolds with similar thickness, the size of the collecting surface was controlled by using aluminum foils with the same surface area to cover the surfaces of the conductive plate or rotating drum before the collections, and the collecting time for all samples was fixed for 30 min.

To characterize the nanofiber alignment of the electrospun scaffolds with different aligned patterns, the values of order degree were calculated according to the following equation:[24−26]

$$S = 2\cos^2\theta - 1 \quad (1)$$

where θ is the average angle between the random nanofiber orientation and the preferred alignment direction. Theoretically, the value of S is 0 when the nanofiber arrangement is completely random, while S is 1 for all nanofibers with perfect alignment.

All of the experiments were conducted at room temperature, and the relative humidity was about 40−60%, and all of the as-prepared electrospun scaffolds were vacuum-dried for 24 h to completely remove the residual solvent prior to further characterization.

2.3. Microstructure, Mechanical Properties, and Surface Wettability of the Electrospun Scaffolds with Anisotropically Aligned Patterns. The morphology and microstructure of the electrospun scaffolds were observed using an optical microscope (Leica DM2500 M) and an environment scanning electron microscope (SEM, FEI, QUANTA 250, The Netherlands) operated at an accelerating voltage of 10 kV.

To investigate the mechanical strengths of the prepared scaffolds, the tensile tests of the electrospun scaffolds were conducted using an Autograph AG-5kNX mechanical testing machine (Shimadzu) according to Japanese Industrial Standards (JIS) K 7161. In this process, the samples were cut into rectangular strips with an average area of 50 × 10 mm^2. The specimens were gripped by two tensile fixtures with a gauge length of about 20 mm, and the cross-head speed for the tensile tests was 2 mm min^{-1}. The tensile test of patterned electrospun scaffolds was performed along the direction of parallel nanofibers between embossments (defined as longitudinal (L)) and the direction of embossments (defined as transverse (T)), respectively. At least one group of five samples was used for each test to obtain an average. All tests were performed at room temperature and a relative humidity of about 60%.

For investigating the effect of anisotropically aligned patterns on the surface wettability of the scaffolds, the static water contacting angles (WCA) were measured using a Kruss GmbH DSA 100 Mk 2 goniometer (Hamburg, Germany), followed by image processing of sessile drops using a DataPhysics OCA20 CA system at ambient temperature. Water droplets (3.0 μL) were dropped carefully onto the surfaces of the patterned electrospun scaffolds. The average WCA value was obtained by measuring the water droplets set at 10 randomly distributed positions.

2.4. Cell Culture. Human umbilical vein endothelial cells (HUVECs) were isolated from the human umbilical cord vein according to the descriptions of Bordenave et al. and Jaffe.[27,28] The procedure was approved by the Ethics Committee of Shanghai Jiaotong University. The obtained cell pellets were redispersed in endothelial cell medium (ECM) (Sciencell, U.S.) containing 5% (vol/vol) FBS and 1% (vol/vol) endothelial cell growth supplement/heparin kit (ECGS/H, Promocell). In this study, cells between passages 3 and 5 were employed.

2.5. HUVECs Proliferation Assay. To evaluate the influence of the anisotropically aligned pattern of electrospun nanofibrous scaffolds on cell proliferation, samples were first sectioned into 10 × 10 mm^2 squares, and then cross-linked with glutaraldehyde/ethanol (v/v = 1/1) for 0.5 h. After that, samples were washed out with a large amount of deionized water and soaked in 75 vol % medical alcohol solution for another 2 h for sterilization prior to seeding cells on the samples. HUVECs were seeded on the surfaces of those scaffolds at a density of 1.5×10^4 cells per well in a 24-well culture plate, and then cultured in a humidified 37 °C/5%, CO_2 incubator for 1, 3, and 7 days. Cells cultured with nonwoven, single directionally aligned electrospun scaffolds were regarded as controls. The medium was replaced every 2 days. A CCK-8 assay (Cell counting kit-8, Dojindo, Kumamoto, Japan) was performed according to the manufacturer's instructions. The absorbance of the samples was measured at 450 nm using an enzyme-linked immunosorbent assay plate reader (Synergy 2, Bio-TEK).

2.6. Live/Dead Staining. To evaluate cell viability to the electrospun nanofibrous scaffolds, after being cultured for 7 days, a live/dead viability cytotoxicity kit (Invitrogen) was applied to stain cells according to the supplier's procedure. The cell viability and arrangement on the surfaces of electrospun nanofibrous scaffolds with different patterns were observed and photographed using a CCD camera (Leica DFC 420C) equipped with a fluorescence microscope (Leica DM2500 M).

2.7. Immunofluorescence Staining. For further investigating the cytoskeletal and nuclear organizations of HUVECs cultured on different scaffolds, the actin filaments and nuclear of HUVECs were stained utilizing rodamine phalloidin R415 (Invitrogen) and 4−6-diamidino-2-phenylindole (DAPI) (Invitrogen) according to the supplier's procedure, respectively. A confocal microscope (Leica TCS SP5) was used to image the morphologies of the seeded cells as a function of scaffold architecture, and the cell area and perimeter were measured by the measure tool in ImageJ software. The cell morphology was further characterized by cell shape index, which was calculated according to the following equation:[29,30]

DOI: 10.1021/acsami.5b00996
ACS Appl. Mater. Interfaces 2015, 7, 8706−8718

Table 1. Primer Sequences Used in Q-RT-PCR

gene	gene bank	primer sequences	T_m (°C)
$VEGF_{165}$	AB_021221	F:5′-TGCGGATCAAACCTCACCA-3′	58
		R:5′-CAGGGATTTTTCTTGTCTTGCT-3′	
KDR	NM_002253	F:5′-GTGATCGGAAATGACACTGGAG-3′	60
		R:5′-CATGTTGGTCACTAACAGAAGCA-3′	
eNOS	NM_001160111.1	F:5′-TGTCCAACATGCTGCTGGAAATTG-3′	55
		R:5′-AGGAGGTCTTCTTCCTGGTGATGCC-3′	
VE-cad	NM_001795	F:5′-GGCTCAGACATCCACATAACC-3′	63
		R:5′-CTTACCAGGGCGTTCAGGGAC-3′	
GAPDH	NM_002046	F:50-GATTTGGTCGTATTGGGCG-30	60
		R:50-CTGGAAGATGGTGATGG-30	

$$I_n = 4\pi S/L^2 \quad (2)$$

where I is the value of a cell body shape index, and S and L are the cellular area and perimeter, respectively. The cell is round when I is equal to 1, and the cell becomes infinitely elongated as I approaches 0. About 100 cells for one local region with special microstructure in scaffolds were analyzed, and the obtained average value (I_n) represents the body shape index for cells in the corresponding local region.

On the basis of these, the mean cell body shape index for cells in a whole scaffold (I_w) was further determined using the following equation:

$$I_w = (I_1N_1 + I_2N_2 + ... + I_nN_n)/(N_1 + N_2 + ...N_n) \quad (3)$$

where I_1, I_2, I_n are the values of the cell body shape index in different local regions with special microstructure in scaffolds, and N_1, N_2, N_n are the number of cells in the corresponding local regions, respectively. Using this method, the mean cell body shape index for cells in scaffolds with anisotropically aligned pattern as well as nonwoven and single directionally aligned structure was further investigated.

2.8. Quantitative Real-Time Polymerase Chain Reaction (Q-RT-PCR). To investigate the effect of anisotropically aligned patterns on the differentiation of HUVECs, gene expression of vascular endothelial growth factor (VEGF), VEGF receptor 2 (KDR), endothelial nitric oxide synthase (eNOS), and vascular endothelial vadherin (VE-cad) from the cells cultured on different scaffolds for 7 days was detected by quantitative real-time polymerase chain reaction (Q-RT-PCR). For RNA extraction, at the determined time point, cells were washed twice with cold phosphate buffered saline (PBS), and the total RNA was prepared from cells using an E. Z. N. A Total RNA kit I (OMEGA, Biotek) according to the manufacturer's guidelines. The concentration of RNA was measured using a nanodrop 1000 reader (Thermo Scientific). cDNA was synthesized using a ReverTra Ace-a kit (Toyobo, Japan) according to the instructions. One microliter of cDNA, which was diluted at 1:10 in sterilized Mill-Q water, was mixed with 9 μL of SYBR-Green. Primers of VEGF, KDR, eNOS, and VE-cad (all from Sangon Biotech (Shanghai)) were used as the final concentration of 400 nM. Glyceraldehyde 3-phosphate dehydrogenase (GAPDH) was used as a housekeeping gene. Their sequences are summarized in Table 1. Real-time PCR Master Mix (Toyobo) containing primers were loaded in a 384-well plate. Real-time PCR analysis was performed using the 7900 Real-time PCR system (Applied Biosystems). After an initial incubation step of denaturation for 1 min at 95 °C, 40 cycles (95 °C for 15 s, 60 °C for 15 s, 72 °C for 45 s) of PCR were performed. Reactions were performed in triplicate. Data were analyzed with the SDS 2.3 software and compared using the ΔΔCt method, and each Q-RT-PCR was performed in triplicate for Q-RT-PCR yield validation. Data were normalized to GAPDH mRNA expression of each condition and were quantified relative to the corresponding gene expression from the control samples (cell cultured on the surface of nonwoven electrospun nanofibrous scaffolds), which were standardized to 1.

2.9. Statistical Analysis. The results were expressed as the arithmetic mean ± standard deviation. Three independent experiments were carried out, and at least five samples per each test were taken for statistical analysis. Statistical significance between two groups was calculated using two-tailed analysis of variance (ANOVA) and performed with a Student's t test program. Differences were considered significant when $p < 0.05$ (*), $p < 0.01$ (**), or $p < 0.001$ (***). In addition, a one-way ANOVA with Tukey's post hoc test was used for statistical analysis of multiple comparisons. Significant difference was considered when $p < 0.05$ (*), $p < 0.01$ (**), or $p < 0.001$ (***).

3. RESULTS

3.1. Microstructure of Electrospun Nanofibrous Scaffolds with Anisotropically Aligned Patterns. Figure 1A shows the electrospun scaffolds with various structures prepared with different collecting devices. The optical microscopic images of scaffolds are shown in Figure 1A(a−e), and the corresponding SEM images are shown in Figure 1A(a1−e1), respectively. Figure 1A(a) and (a1) shows the electrospun scaffold prepared using a flat collector during the process of electrospinning. As observed from the optical microscopic image, a scaffold with tightly packed two-dimensional (2D) sheet-like structure was generated after the electrospinning process. From the corresponding SEM image, it is clear to see that the nanofibers are randomly deposited in an interwoven network structure and the average diameter of nanofibers is 500−700 nm. Similar to the scaffolds collected with a flat collector, the electrospun nanofibrous scaffolds collected with a rotating drum system shown in Figure 1A(b) exhibit a uniform and dense feature. However, different from the random arrangement of nanofibers observed in Figure 1A(a1), nanofibers in the scaffolds collected with rotating drum are aligned in a single direction (Figure 1A(b1)).

In contrast to those random or single directionally aligned nanofibers, scaffolds prepared using a wire spring as a template collector show well-organized topological structures with anisotropically and heterogeneously aligned patterns, and the schematic illustration of the template-assisted collection process is shown in Figure 1B. Figure 1A(c−e) shows the optical images of patterned scaffolds. A distinct difference in nanofiber density in different regions of scaffolds can be seen: the density of nanofibers deposited on the embossments is higher than that of the nanofibers suspended between the embossments. SEM images of scaffolds collected through wire springs with intervals distances of 300, 800, and 1500 μm are shown in Figure 1A(c1,c1′), (d1,d1′), and (e1,e1′), respectively. From these images, it can be seen that nanofibers deposited on the embossments are randomly distributed, while those nanofibers suspended between the embossments are tending to arrange in a parallel manner. As a result, a patterned scaffold with spatially heterogeneous fiber alignment was generated, in which some regions were anisotropic. Nanofibers deposited on the embossments are shown in (c2,c2′), (d2,d2′), and (e2,e2′),

DOI: 10.1021/acsami.5b00996
ACS Appl. Mater. Interfaces 2015, 7, 8706−8718

Table 2. Order Degree of the Different Aligned Structures within the Patterned Electrospun Scaffolds

			micropattern (300 μm)		800 μm		1500 μm	
	nonwoven	aligned	longitudinal (L)	transverse (T)	L	T	L	T
$\overline{\theta}$ (deg)	34.285	4.843	3.275	34.761	3.525	37.727	2.461	40.501
order degree (S)	0.365	0.986	0.993	0.350	0.992	0.251	0.996	0.156

respectively. As observed, a large number of nanofibers are assembled on the embossments and formed into a cylindrical-like structure (c2−e2). SEM images with high magnification show that nanofibers randomly deposited on the embossments with high density and formed into a compact structure (c2′−e2′), which is different from the loose and porous three-dimensional (3D) nanofibrous structure formed by suspended aligned fibers between embossments (c1′−e1′). In addition, the order degree of the electrospun scaffolds with different aligned patterns was calculated. As shown in Table 2, the nanofibers suspended between the embossments possess an extremely high value of order degree, which is similar to that of the single directionally aligned electrospun scaffolds; meanwhile, the nanofibers assembled on the embossments of patterned scaffolds show a relatively lower value of order degree, while the scaffolds with nonwoven structures are in the same situation. In addition, these results also confirm the fact that the interval distance between embossments has no obvious effect on the nanofiber deposition and patterns.

3.2. Effect of Anisotropically Aligned Patterns on Surface Wettability and Mechanical Properties of Electrospun Nanofibrous Scaffolds. The surface wettability of the electrospun scaffolds with different arrangements of nanofibers was investigated by water contact angle measurements, and the results are shown in Figure 2. As observed, the

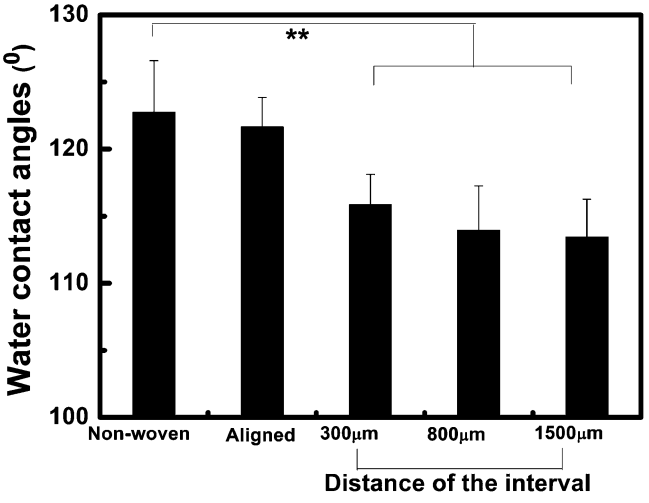

Figure 2. Water contact angles of electrospun nanofibrous scaffolds with different aligned patterns (** represents $p < 0.01$).

nonwoven electrospun scaffold has a highest water contact angle of 122.8° ± 3.79°, which is essentially hydrophobic, and the electrospun scaffolds with single directionally aligned pattern show a water contact angle similar to that of the nonwoven scaffolds. In contrast, three anisotropically patterned scaffolds tended to have much lower water contact angles (~113° ± 2.76°) than those of nonwoven and single directionally aligned scaffolds. However, there is no obvious difference among the three patterned scaffolds with varied interval distances between embossments (Figure 2).

The tensile strengths and elastic moduli in both the longitudinal (L) and the transverse (T) directions of electrospun nanofibrous scaffolds with different aligned patterns are shown in Figure 3A and B, respectively. The electrospun scaffolds with nonwoven nanofibers show mechanical isotropy as their tensile strengths and elastic moduli in both the L and the T directions are nearly identical. However, the nanofibrous scaffolds with single directionally aligned nanofibers exhibit mechanical anisotropy as their tensile strengths and elastic moduli in the L directions are greatly higher than those in the T directions. Interestingly, the electrospun scaffolds with anisotropically aligned patterned nanofibers show mechanical properties between isotropy and anisotropy as their tensile strengths and elastic moduli in the L and T directions are significantly different, but the direction with superior mechanical properties can be changed by the interval distance between embossments. With the decrease of interval distance, the tensile strengths and elastic moduli in the L direction are significantly decreased, while the ones in T direction gradually increased. When the interval distance is as long as 1500 μm, the tensile strengths of patterned scaffold in L and T directions are 1.75 and 0.54 MPa (Figure 3A), while the corresponding elastic moduli are 5.27 and 1.54 MPa (Figure 3B), respectively.

3.3. Effect of Anisotropically Aligned Patterns on Cell Proliferation and Distribution. The proliferation behaviors of HUVECs on the scaffolds with different aligned patterns are shown in Figure 4. After 1 day of culture, the number of HUVECs in the scaffolds with anisotropically aligned patterns is higher than that in the nonwoven or single directionally aligned scaffolds. With culture time increasing, all scaffolds can support HUVECs growth. However, after 7 days, the number of HUVECs cultured on scaffolds with anisotropically aligned patterns is much higher than those cultured on nonwoven and single directionally aligned scaffolds, which indicates that the scaffolds with anisotropically aligned patterns have stimulatory effects on HUVEC proliferation.

After 7 days of culture, the viability and distribution of HUVECs on all electrospun scaffolds were observed using a florescence microscope, and the images are shown in Figure 5. It is clear to see that HUVECs attached and grew well on all electrospun scaffolds. HUVECs evenly distributed on both the nonwoven and the single directionally aligned scaffolds. On the nonwoven scaffolds, cells spread toward different directions (Figure 5A). In contrast, cells grew along the direction of the fiber arrangement on the single directionally aligned scaffolds (Figure 5B). Unlike the even distribution of the cells on these two kinds of scaffolds, HUVECs in different regions of anisotropically aligned patterned scaffolds show quite different distributions. The cells are found to align and organize under the guidance of the micropatterned constructs of underlying scaffolds (Figure 5C−E). In the intervals between embossments of anisotropically patterned electrospun scaffolds, a guided growth with cell polarity following the aligned fiber

DOI: 10.1021/acsami.5b00996
ACS Appl. Mater. Interfaces 2015, 7, 8706−8718

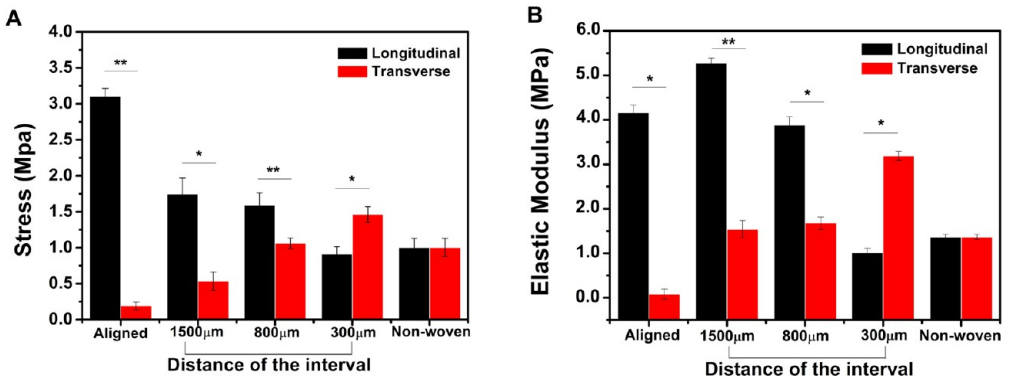

Figure 3. Tensile strengths (A) and elastic moduli (B) of electrospun nanofibrous scaffolds with different aligned patterns (* represents $p < 0.05$ and ** represents $p < 0.01$).

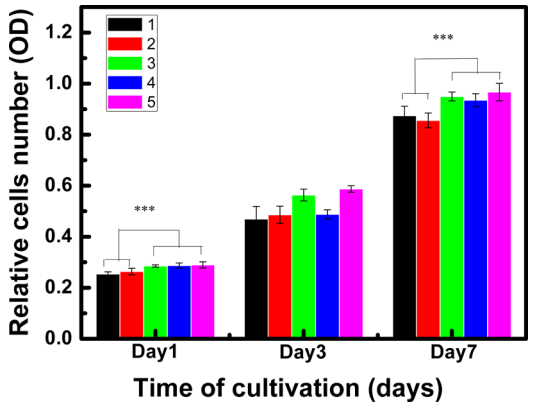

Figure 4. Proliferation of HUVECs on electrospun scaffolds with different aligned patterns: (1) nonwoven; (2) single directionally aligned pattern; (3−5) anisotropically aligned patterns with distances of intervals 300, 800, and 1500 μm, respectively (*** represents $p < 0.001$).

direction is clearly evident (Figure 5C1−E1), while the cells on the embossments of scaffolds gathered together to form cylindrical-like cell layers without directional elongation (Figure 5C2−E2).

3.4. Effect of Anisotropically Aligned Patterns on the Cell Cytoskeleton and Nuclei Organizations. Cytoskeleton organizations of HUVECs grown on the surfaces with different aligned patterns were investigated after 7 days of cell culture. As shown in Figure 6, HUVECs adapted their cytoskeleton morphologies on electrospun scaffolds with different microstructures. HUVECs exhibited a typical cobblestone-like structure on the culture plate (Figure 6O). When cultured on the surfaces of nonwoven electrospun scaffolds, the cells were flattened and showed round shape morphology (Figure 6A), while some of the HUVECs in the single directionally aligned scaffolds elongated along the direction of nanofibers (Figure 6B). Interestingly, cells in different regions of anisotropically aligned patterned scaffolds presented different morphologies. As shown in Figure 6C1−E1, the cells grew uniformly along the direction of the fiber arrangement on the suspended nanofibers between the embossments of scaffolds. Under high magnifications, the cells are observed to show a spindle shape along the long axes (Figure 6C1′−E1′). As compared to the cell alignment on the single directionally aligned scaffolds, higher alignment degree of HUVECs can be observed on the anisotropically patterned scaffolds. Meanwhile, the cells on the embossments of anisotropically patterned scaffolds exhibited a polygonal shape with stretching in random directions (Figure 6C2′−E2′).

The quantitative analysis of the body elongation of HUVECs in different local regions with special microstructures in scaffolds was conducted. As shown in Figure 7A, cells in the regions with different aligned structures show lower shape index as compared to that in the regions with nonwoven structures in scaffolds, and the shape index of the cells in the regions with suspended aligned nanofibers between the embossments of patterned scaffolds is the lowest as compared to cells in other regions. In addition, it is also noticed that the cells seeded on the embossments of the patterned scaffolds possess a relatively lower shape index than that in regions with nonwoven structures. Moreover, the cells on the scaffolds with anisotropically aligned patterns present significantly lower mean shape index than those on the nonwoven scaffolds (Figure 7B), and a significant drop in the mean shape index of HUVECs could be observed with the increase of the interval distance in micropatterns, and the patterned scaffolds with the longest distance of interval (1500 μm) have the lowest mean cell shape index.

Nuclear organizations of HUVECs grown on different aligned patterns were investigated after 7 days of cell culture. Nuclei of HUVECs distributed on the nonwoven scaffolds randomly show no polarization (Figure 8A), while some nuclei of HUVECs cultured on the single directionally aligned scaffolds elongated along the direction of nanofibers (Figure 8B). However, nuclei of HUVECs cultured in different regions of patterned scaffolds show different morphologies. Nuclei of HUVECs on the suspended aligned nanofibers in the regions between embossments exhibited an obvious long oval shape with the long axes parallel to each other (Figure 8C1−E1 and C1′−E1′). In addition, the nuclei elongation of HUVECs cultured on the suspended aligned nanofibers in the scaffolds with anisotropically aligned patterns is more apparent than that cultured on nonwoven or single directionally aligned scaffolds. Meanwhile, the nuclei of HUVECs cultured on the embossments of scaffolds display a round shape with random distribution directions, which are similar to those on the nonwoven scaffolds (Figure 8C2−E2 and C2′−E2′).

3.5. Effect of Anisotropically Aligned Patterns on Angiogenesis Related Gene Expression. Expression of VEGF, KDR, eNOS, and VE-Cadherin from HUVECs cultured on scaffolds with different aligned patterns has been investigated. As shown in Figure 9, expression levels of

DOI: 10.1021/acsami.5b00996
ACS Appl. Mater. Interfaces 2015, 7, 8706−8718

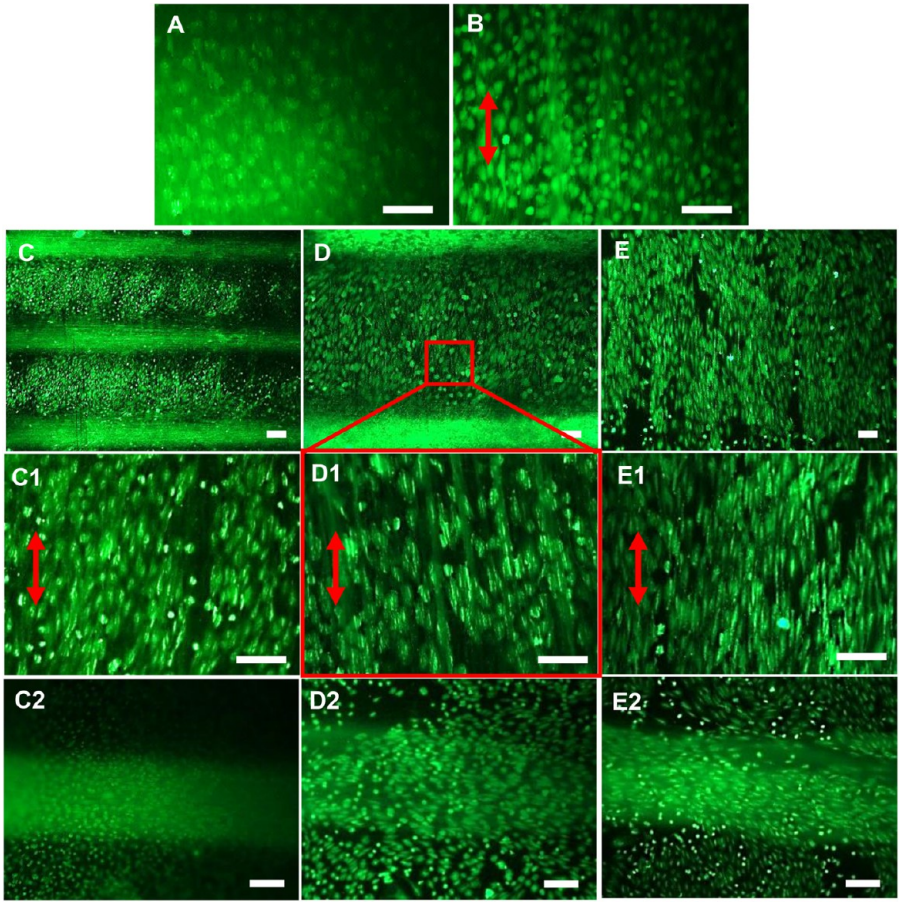

Figure 5. Live/dead staining of HUVECs after 7 days growth on electrospun scaffolds with different aligned patterns, in which green indicates live cells and dead cells could be stained in red. The results showed that all cells are green stained and no dead cells were observed. (A) Nonwoven; (B) single directionally aligned pattern; (C–E) anisotropically aligned patterns with distance intervals of 300, 800, and 1500 μm, respectively. The cell shape and arrangement on the aligned nanofibers between the embossments in (C–E) are shown in (C1–E1), while the cell shape and arrangement on the nanofibers deposited on the embossments are shown in (C2–E2), respectively (scale bar = 100 μm).

angiogenesis-related genes, such as VEGF (Figure 9A), KDR (Figure 9B), eNOS (Figure 9C), and VE-Cadherin (Figure 9D), from HUVECs cultured on the anisotropically aligned patterned electrospun scaffolds are much higher than those from HUVECs cultured on the nonwoven scaffolds. In addition, it is found that the interval distance of the patterns in the scaffolds plays an important role in influencing those gene expressions of HUVECs. Cells cultured in the patterned scaffolds with the longest distance of interval (1500 μm) demonstrate the highest level of gene expression than the nonwoven or single directionally aligned scaffolds (Figure 9).

4. DISCUSSION

Currently, the electrospun nanofibers are typically collected randomly in a nonwoven structure as a result of the bending instability associated with the electrified polymeric jets, and the fabrication of scaffolds composed of single directionally aligned nanofibers has also been widely reported as the main topographical control of electrospun materials.[12,13] Herein, we demonstrated an innovative approach based on the modified collecting technique for preparing a new type of electrospun scaffolds with anisotropically and heterogeneously aligned patterns, which can not only provide controlled mechanical properties but also activity to stimulate the proliferation and differentiation of endothelial cells.

It is well-known that the natural blood vessel is an extremely complex multilayered tissue, and each layer plays an integral role in providing adequate mechanical strength to withstand the high flow rate of blood. Especially, it is worth mentioning that the middle layer of the blood vessel makes the main contribution to resist the high pressure of blood pulsation on the radial direction, which benefits from the smooth muscle cells and collagen fibrils arranged in a marked circumferential orientation.[31] Because of these distinct structural organizations of each layer, the blood vessel exhibits a multidirectional mechanical behavior.[32] Therefore, for fabrication of an ideal vascular tissue engineering scaffolds, to mimic the mechanical property of the native blood vessel and achieve effective control of the tensile strengths in multiple directions of the scaffolds is of great importance.

In the present study, a wire spring was introduced as a template collector of electrospinning. As shown in Figure 1, the space between the neighboring convex embossments of the wire spring can be regarded as a tridimensional void gap model,[33] which can alter the configuration of the electrostatic forces acting on the nanofibers spinning across the gap, and the nanofibers thus align into a uniaxial array between the embossments with a porous 3D nanofibrous construct under the action of electrostatic forces in opposite directions. Meanwhile, the nanofibers deposit with a high density on the electroconductive embossment with a compact cylindrical-like

DOI: 10.1021/acsami.5b00996
ACS Appl. Mater. Interfaces 2015, 7, 8706–8718

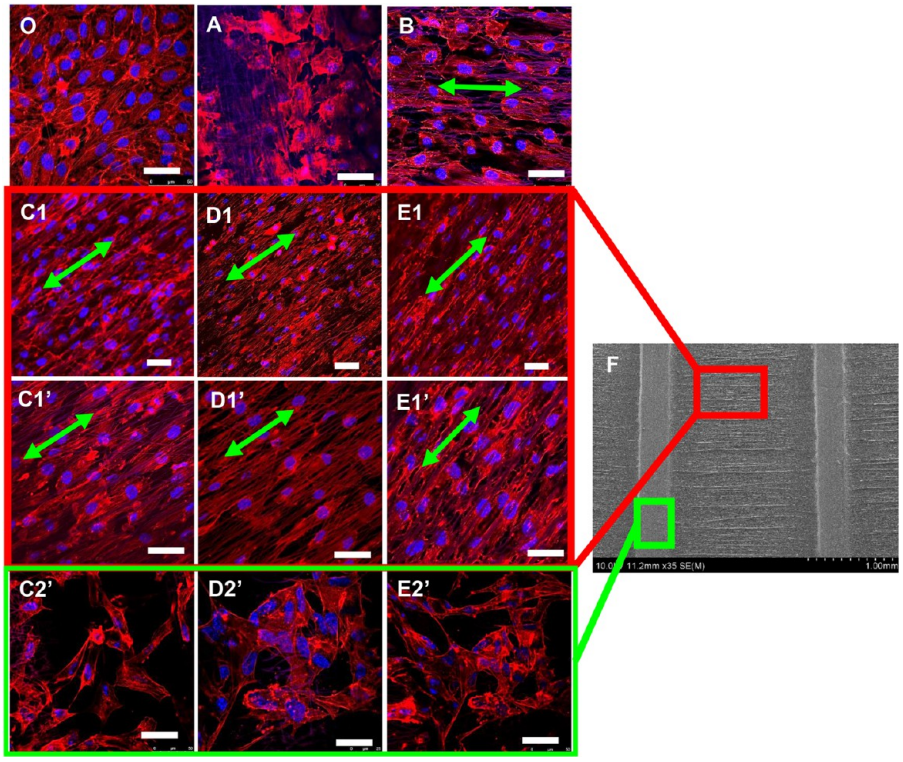

Figure 6. Cytoskeleton organizations of HUVECs after being cultured for 7 days on electrospun scaffolds with different aligned patterns: (A) nonwoven; (B) single directionally aligned pattern; (C1−E1) aligned nanofibers between the embossments in the anisotropically aligned patterns, which possess interval distances of 300, 800, and 1500 μm, respectively, and (C1′−E1′) are the corresponding higher magnification images of (C1−E1), respectively; (C2′−E2′) show cells on the embossments in the anisotropically aligned pattern (as shown in (F)). (F) A typical SEM image of anisotropically aligned pattern. Part (O) shows the cytoskeleton organizations of HUVECs after 7 days growth on a culture plate (scale bar = 50 μm).

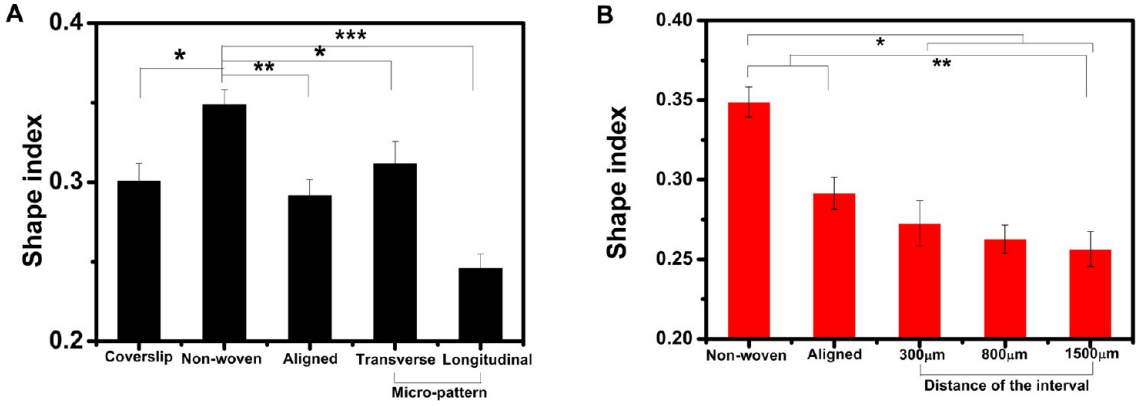

Figure 7. Cell body shape index of HUVECs after being cultured for 7 days on (A) different local regions with special microstructures in scaffolds and (B) scaffolds with different aligned patterns (*, **, and *** represent $p < 0.05$, $p < 0.01$, and $p < 0.001$, respectively).

structure, where the electric field is more intense as compared to the area between embossments. As a result, electrospun scaffolds with anisotropically and heterogeneously aligned patterns containing multiple structural features were successfully fabricated, and the mechanical test results demonstrated that the electrospun scaffolds with anisotropically aligned patterns can furthest imitate the multidirectional mechanical behaviors of native vessels, as the tensile strengths and elastic moduli in both longitudinal and radial directions of the scaffolds could be efficiently controlled by controlling well-defined fibrous patterns. Wang et al. have demonstrated that the orientation of nanofibers largely affected the mechanical behaviors of electrospun scaffolds as when the fiber orientation increased, the nanofibrous scaffolds showed a significantly increased tensile strength along the fiber direction, and the tensile strength of parallel nanofibers along the fiber direction was approximately 3 times that of the randomly arranged fibers.[34] Consistent with the previous studies, similar tensile strength differentials between the nonwoven and single directionally aligned scaffolds in the present work are observed. However, unlike the previous studies, we took a further investigation on the tensile strengths and elastic moduli of electrospun scaffolds not only in the longitudinal direction but also in the transverse direction. The results demonstrated that the nonwoven scaffolds exhibited mechanical isotropy with nearly identical tensile strengths and elastic moduli in both the

DOI: 10.1021/acsami.5b00996
ACS Appl. Mater. Interfaces 2015, 7, 8706−8718

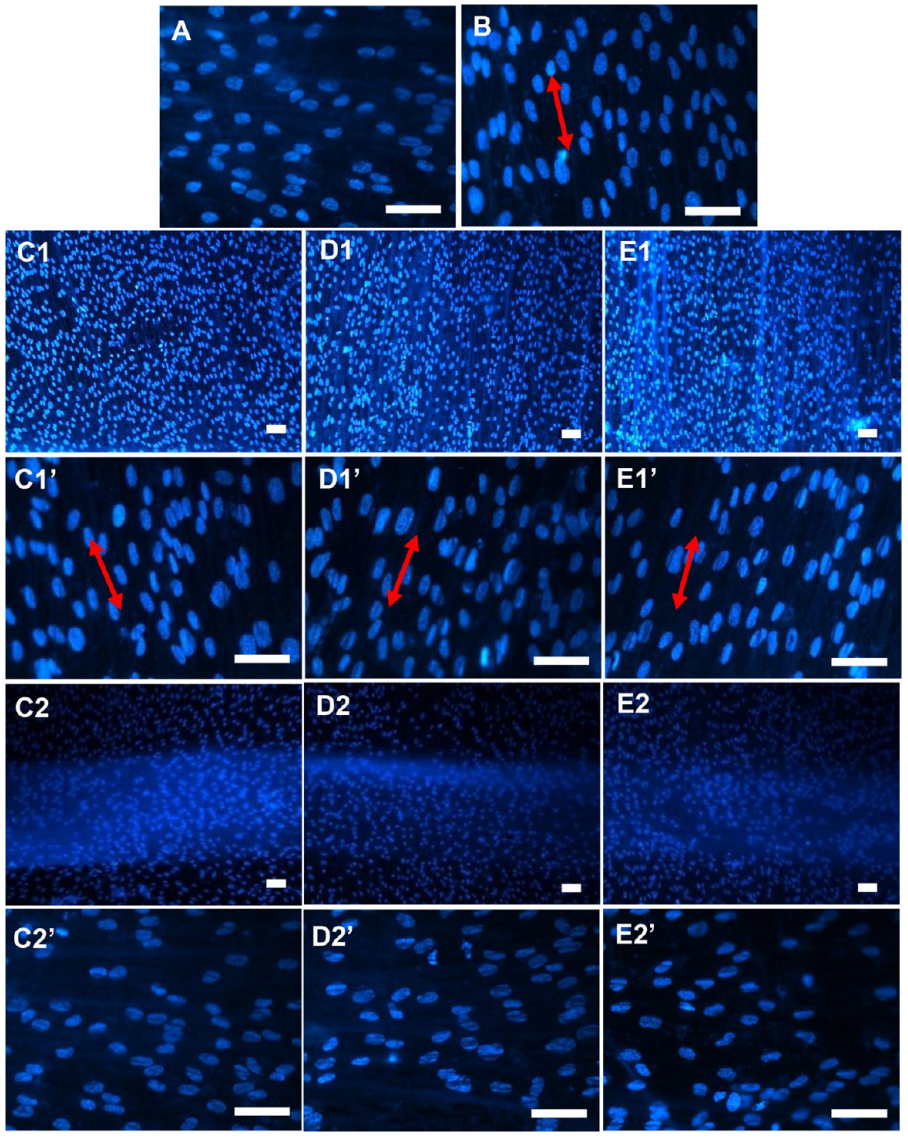

Figure 8. Nuclei morphology of HUVECs cultured for 7 days on electrospun scaffolds with different aligned patterns: (A) nonwoven; (B) single directionally aligned pattern; (C1−E1) aligned nanofibers between the embossments in the anisotropically aligned pattern, which possess the interval distances of 300, 800, and 1500 μm, respectively. (C1′−E1′) show the nuclei morphology of HUVECs cultured in the same regions (higher magnifications); correspondingly, (C2−E2) (low magnification) and (C2′−E2′) (high magnification) are the images of nuclei of HUVECs cultured on the embossments in the anisotropically aligned pattern (scale bar = 50 μm).

L and the T directions, which is mainly due to the uniform distribution of fibers in each direction. Meanwhile, the single directionally aligned scaffolds possess significant high tensile strengths and elastic moduli in the direction of nanofiber alignment as a result of the good alignments of nanofibers along this direction. However, low tensile strengths and elastic moduli in the perpendicular direction to the fiber alignment direction was observed, which could be attributed to the weak connection between the neighboring parallel fibers. In contrast, for the scaffolds obtained in the present work with anisotropically aligned pattern, the aligned nanofiber suspended between the embossments is able to withstand the force along the L direction. In addition, the emergence of compact cylindrical-like structure can disperse the stress from the T direction, resulting in an improved tensile strength and elastic modulus in that direction, which is quite different from those of the nonwoven or single directionally aligned electrospun scaffolds. Furthermore, our method also provides an effective way to control the tensile strengths and elastic modulus in the two directions by adjusting the distance of intervals between two embossments, which is very important to meet the requirements of vascular scaffolds with varied mechanical strength for specific clinical applications. Holzapfel et al. have reported that the ultimate tensile stresses of adventitia in human coronary arteries were 1300 and 1430 kPa in the longitudinal and circumferential orientations, respectively.[35] Ozolanta et al. have also reported that the elastic moduli of coronary arteries of males were in the rage of 1.06−4.11 MPa.[36] In our work, the longitudinal tensile strengths of the anisotropically aligned patterned electrospun scaffolds are in the range of 0.911−1.746 MPa and the transverse ones are between 0.536−1.463 MPa, while the corresponding elastic moduli are 1.008−5.27 and 1.54−3.188 MPa, respectively, which are in the ranges of those of the native tissues.

Besides the controlled mechanical properties, the structural effects of the electrospun scaffolds on cell behavior should not

DOI: 10.1021/acsami.5b00996
ACS Appl. Mater. Interfaces 2015, 7, 8706−8718

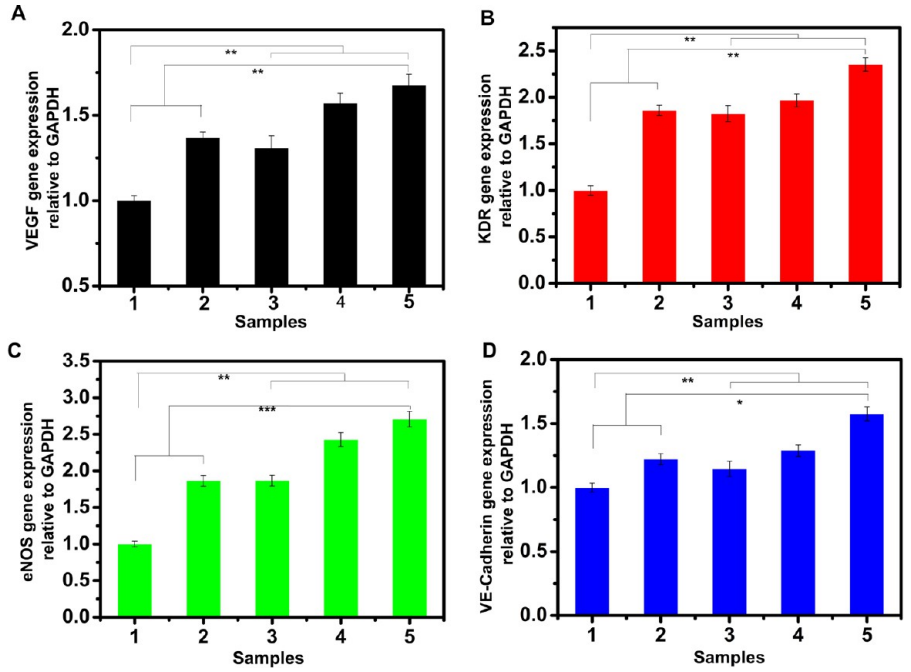

Figure 9. Expressions of angiogenesis-related genes in HUVECs after being cultured for 7 days on electrospun scaffolds with different aligned patterns: (1) nonwoven; (2) single directionally aligned pattern; (3−5) anisotropically aligned patterns with distances of intervals of 300, 800, and 1500 μm, respectively. The corresponding gene expression in HUVECs shown in each panel is (A) VEGF, (B) KDR, (C) eNOS, and (D) VE-Cadherin, respectively (* represents $p < 0.05$, and ** represents $p < 0.01$).

be neglected. Various studies have demonstrated that the fiber orientation of electrospun scaffolds had a significant impact on directing the alignment and elongation of endothelial cells (ECs), which could be regarded as the phenomenon of contact guidance.[12] Whited et al. took a further investigation on the structural protein organization of ECs on an aligned PCL electrospun scaffold, and the results showed that endothelium cells on aligned electrospun scaffolds displayed thick F-actin bundles parallel to the direction of fiber alignment and strong VE-cadherin expression at cell−cell junctions.[37] All of those studies have proved that the microstructures of scaffolds play vital roles in influencing the ECs behaviors, which is of great importance to construct tissue engineered blood vessels.

Sun et al. have already demonstrated that the cell attachment and migration would be greatly influenced by the diameter of electrospun fibers.[38] In this work, our aim is to investigate the effect of the fibrous patterns on cells, so attention has been paid to fabricating electrospun nanofibers with similar diameters for all samples by controlling the experimental conditions to eliminate the effect of the fiber diameters. Our results showed that the well-designed scaffolds with anisotropically and heterogeneously aligned patterns could significantly promote ECs adhesion at the early stage and proliferation during the culture period. Meanwhile, the traditional nonwoven or single directionally aligned scaffolds possess a relatively lower cell proliferation, which is mainly due to the tightly packed sheet-like shapes with uncontrollable microstructures.[39] In addition, WCAs measurement results revealed that the scaffolds with anisotropically aligned patterns showed higher hydrophilicity as compared to the nonwoven or single directionally aligned nanofibers, which is mainly due to the altered nanofiber density distribution on the surfaces of patterned scaffolds.[40] The aligned nanofibers suspended between embossments have a much lower fiber density and present low hydrophobicity, which can significantly improve cell adhesion at the early stage. Furthermore, the suspended aligned nanofiber bundles in this region construct a loose 3D structural microenvironment, which may be beneficial to supply oxygen and nutrient to cells and finally induce a relatively high proliferation and good cell viability.

Moreover, another important finding in our study is that the micropatterned scaffolds could significantly promote the angiogenic differentiation of HUVECs. When HUVECs were cultured on scaffolds with different structures, the cells aligned and organized within the micropatterned constructs of underlying scaffolds. Meanwhile, the cell shape varied and associated with cell cytoskeleton and nuclei remodeling as a result of the morphological restriction by micropatterns. It has been widely reported that the remodeling of cell cytoskeleton and nuclei plays a significant role in the regulation of cellular differentiation, as the coupling cytoskeletal/nuclear alterations could modulate the chromosomal architecture and dynamic positioning in the nuclear space, which will regulate the subsequent accession of transcription factors to their target genes.[41,42]

To further elucidate how the micropatterns affect the shapes and angiogenesis-related gene expression of cells, quantitative analysis of the body elongation of HUVECs in different local regions with special microstructures in scaffolds was conducted. As the lower shape index means higher elongation of cell bodies,[29] our results suggest that the cell elongation in the regions with suspended aligned nanofibers between the embossments of patterned scaffolds is more distinct than that in other regions. As compared to the regions of single directionally aligned structure in tightly packed 2D sheet-like scaffolds, the regions with suspended aligned fibers between embossments have a lower fiber density and exhibit a loose 3D nanofibrous microenvironment. Therefore, the cells in these regions may catch fewer fibers in the transverse direction than that for cells in the regions with single aligned structures, so the

DOI: 10.1021/acsami.5b00996
ACS Appl. Mater. Interfaces 2015, 7, 8706−8718

directional effect of aligned structures is much stronger for the cells in regions with suspended aligned fibers between embossments, which will result in more obvious elongation of cell body along the fiber direction,[43] as schematically illustrated in Figure 10B and C. In addition, it is noticed that

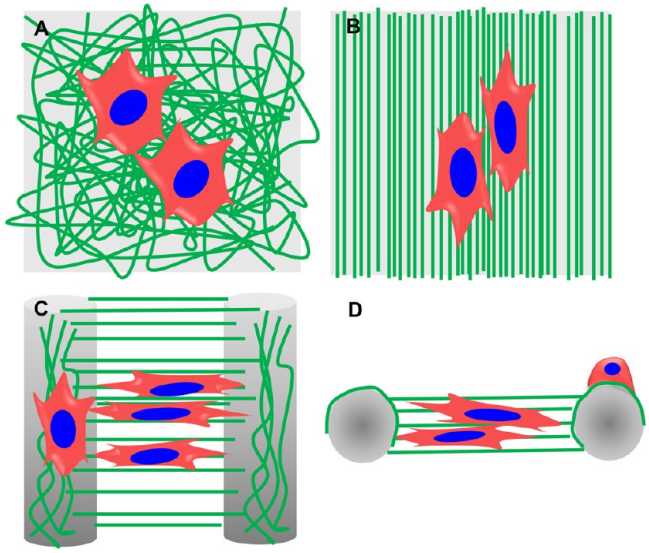

Figure 10. Schematic mechanism illustration of the cell morphologies on electrospun membranes with different aligned pattern: (A) nonwoven; (B) single directionally aligned pattern; (C) anisotropically aligned patterns (top view); and (D) anisotropically aligned patterns (front view).

the cells seeded on the embossments of the patterned scaffolds possess a relatively higher degree of elongation than that in regions with nonwoven structures. The possible explanation is that, as the electric force acting on the fibers is directed preferentially toward the highest points of the convex embossments, the fibers deposited on the embossments with a gradient variation of fiber density and the highest points of embossments possess the maximum fiber density.[44] Therefore, the embossments possess a relatively uneven surface as compared to the regions with nonwoven structures. Cells cultured in these regions are affected by the surface with a gradient density, resulting in the cellular polarization to a certain degree (Figure 10D) as compared to cells in regions with nonwoven structures (Figure 10A).[45]

The mean cell body shape index is a parameter reflecting the degree of cell polarization on a whole scaffold.[29] Notably, the cells on the scaffolds with anisotropically aligned structures present a significantly higher degree of cell polarization than those on the nonwoven scaffolds, and the interval distance in micropatterns seems to have an obvious effect on the body shape index of HUVECs. Interestingly, the quantitative analysis of mean cell shape index is well correlated with the expression of angiogenesis related genes of HUVECs. The HUVECs on the scaffolds with lower shape index lead to a higher level of gene expression. Lei et al. have also demonstrated that the ECs with larger elongation on the narrower stripes of patterned substrates resulted in the formation of the central lumen of tubular structures as compared to those with smaller elongation on the wider stripes.[21] Consistent with their studies, the patterned scaffolds with the longest distance of interval (1500 μm), which have the lowest mean cell shape index and largest cellular shape change among all scaffolds, showed the highest stimulatory effects on angiogenesis-related gene expression of HUVECs.

Overall, our results suggest that the microstructures of electrospun scaffolds could change the cell body shape index and further regulate angiogenic differentiation of HUVECs for potential vascular tissue engineering application. However, we need to bear in mind in designing scaffolds that mechanical strength is another factor that determines the overall properties of the scaffolds, and we have found that the radial tensile strength of patterned scaffolds decreased with increase of the distance of interval, and the radial tensile strength of patterned scaffold is 0.54 MPa when the interval distance is 1500 μm, which is lower than that of most of the natural vascular tissue.[46,47] Therefore, a balance between the mechanical strength and biological activity of the scaffold needs to be considered, and 1500 μm distance of interval might be the uplimit for patterned scaffolds.

5. CONCLUSIONS

In this work, 3D electrospun scaffolds with anisotropically and heterogeneously aligned patterns were successfully fabricated by an innovative approach using unique wire spring templates. Such well-designed patterned microstructures could not only effectively control the tensile strengths and elastic modulis of scaffolds in both longitudinal and radial directions, but also stimulate proliferation of HUVECs in the scaffolds. Most importantly, cells experienced a large shape change associated with cell cytoskeleton and nuclei remodeling, leading to a stimulatory effect on angiogenesis differentiation of HUVECs by the patterned microstructures of electrospun scaffolds, and the scaffolds with larger distances of intervals showed a higher stimulatory effect. Our results suggest that electrospun scaffolds with the anisotropically and heterogeneously aligned patterns, which could efficiently control the mechanical properties and bioactivities of the scaffolds, might have great potential in vascular tissue engineering application.

AUTHOR INFORMATION

Corresponding Author

*Tel.: +86-21-52412804. Fax: +86-21-52413903. E-mail: jchang@mail.sic.ac.cn.

Notes

The authors declare no competing financial interest.

ACKNOWLEDGMENTS

We thank the National Natural Science Foundation of China (Grant nos. 81190132, and 31200714), the Nature Science Foundation of Shanghai Municipal (Grant no. 12ZR1413900), the Innovation Program of Shanghai Municipal Education Commission (Grant no. 14ZZ032), and the Shanghai Pujiang Talent Program (Grant no. 13PJ1404100).

REFERENCES

(1) Andukuri, A.; Kushwaha, M.; Tambralli, A.; Anderson, J. M.; Dean, D. R.; Berry, J. L.; Sohn, Y. D.; Yoon, Y. S.; Brott, B. C.; Jun, H. W. A Hybrid Biomimetic Nanomatrix Composed of Electrospun Polycaprolactone and Bioactive Peptide Amphiphiles for Cardiovascular Implants. *Acta Biomater.* **2011**, *7*, 225−233.

(2) Gaudio, C. D.; Fioravanzo, L.; Folin, M.; Marchi, F.; Ercolani, E.; Bianco, A. Electrospun Tubular Scaffolds: on the Effectiveness of Blending Poly(epsilon-caprolactone) with Poly(3-hydroxybutyrate-co-3-hydroxyvalerate). *J. Biomed. Mater. Res., Part B* **2012**, *100*, 1883−1898.

DOI: 10.1021/acsami.5b00996
ACS Appl. Mater. Interfaces 2015, 7, 8706−8718

(3) Uttayarat, P.; Perets, A.; Li, M.; Pimton, P.; Stachelek, S. J.; Alferiev, I.; Composto, R. J.; Levy, R. J.; Lelkes, P. I. Micropatterning of Three-dimensional Electrospun Polyurethane Vascular Grafts. *Acta Biomater.* **2010**, *6*, 4229−4237.
(4) Ju, Y. M.; Choi, J. S.; Atala, A.; Yoo, J. J.; Lee, S. J. Bilayered Scaffold for Engineering Cellularized Blood Vessels. *Biomaterials* **2010**, *31*, 4313−4321.
(5) Zhang, X. H.; Baughman, C. B.; Kaplan, D. L. In vitro Evaluation of Electrospun Silk Fibroin Scaffolds for Vascular Cell Growth. *Biomaterials* **2008**, *29*, 2217−2227.
(6) McClure, M. J.; Wolfe, P. S.; Simpson, D. G.; Sell, S. A.; Bowlin, G. L. The Use of Air-flow Impedance to Control Fiber Deposition Patterns during Electrospinning. *Biomaterials* **2012**, *33*, 771−779.
(7) Montero, R. B.; Vial, X.; Nguyen, D. T.; Farhand, S.; Reardon, M.; Pham, S. M.; Tsechpenakis, G.; Andreopoulos, F. M. bFGF-containing Electrospun Gelatin Scaffolds with Controlled Nano-architectural Features for Directed Angiogenesis. *Acta Biomater.* **2012**, *8*, 1778−1791.
(8) Neves, N. M.; Campos, R.; Pedro, A.; Cunha, J.; Macedo, F.; Reis, R. L. Patterning of Polymer Nanofiber Meshes by Electrospinning for Biomedical Applications. *Int. J. Nanomed.* **2007**, *2*, 433−448.
(9) Ku, S. H.; Park, C. B. Human Endothelial Cell Growth on Mussel-inspired Nanofiber Scaffold for Vascular Tissue Engineering. *Biomaterials* **2010**, *31*, 9431−9437.
(10) Zhang, D. M.; Chang, J. Electrospinning of Three-Dimensional Nanofibrous Tubes with Controllable Architectures. *Nano Lett.* **2008**, *8*, 3283−3287.
(11) Xu, H.; Cui, W. G.; Chang, J. Fabrication of Patterned PDLLA/PCL Composite Scaffold by Electrospinning. *J. Appl. Polym. Sci.* **2013**, *127*, 1550−1554.
(12) Xu, C. Y.; Inai, R.; Kotaki, M.; Ramakrishna, S. Aligned Biodegradable Nanofibrous Structure: A Potential Scaffold for Blood Vessel Engineering. *Biomaterials* **2004**, *25*, 877−886.
(13) Gerardo-Nava, J.; Führmann, T.; Klinkhammer, K.; Seiler, N.; Mey, J.; Klee, D.; Möller, M.; Dalton, P. D.; Brook, G. A. Human Neural Cell Interactions with Orientated Electrospun Nanofibers in Vitro. *Nanomedicine* **2009**, *4*, 11−30.
(14) Cho, Y. I.; Choi, J. S.; Jeong, S. Y.; Yoo, H. S. Nerve Growth Factor (NGF)-conjugated Electrospun Nanostructures with Topographical Cues for Neuronal Differentiation of Mesenchymal Stem Cells. *Acta Biomater.* **2010**, *6*, 4725−4733.
(15) Duling, R. R.; Dupaix, R. B.; Katsube, N.; Lannutti, J. Mechanical Characterization of Electrospun Polycaprolactone (PCL): A Potential Scaffold for Tissue Engineering. *J. Biomech. Eng.* **2008**, *130*, 011006−1−13.
(16) Martins, A.; Alves da Silva, M. L.; Faria, S.; Marques, A. P.; Reis, R. L.; Neves, N. M. The Influence of Patterned Nanofiber Meshes on Human Mesenchymal Stem Cell Osteogenesis. *Macromol. Biosci.* **2011**, *11*, 978−987.
(17) Kirmizidis, G.; Birch, M. A. Microfabricated Grooved Substrates Influence Cell-Cell Communication and Osteoblast Differentiation In Vitro. *Tissue Eng., Part A* **2009**, *15*, 1427−1436.
(18) Dalby, M. J.; Gadegaard, N.; Tare, R.; Andar, A.; Riehle, M. O.; Herzyk, P.; Wilkinson, C. D.; Oreffo, R. O. The Control of Human Mesenchymal Cell Differentiation using Nanoscale Symmetry and Disorder. *Nat. Mater.* **2007**, *6*, 997−1003.
(19) Yang, Y.; Kusano, K.; Frei, H.; Rossi, F.; Brunette, D. M.; Putnins, E. E. Microtopographical Regulation of Adult Bone Marrow Progenitor Cells Chondrogenic and Osteogenic Gene and Protein Expressions. *J. Biomed. Mater. Res., Part A* **2010**, *95*, 294−304.
(20) Qi, H.; Du, Y. N.; Wang, L. Y.; Kaji, H.; Bae, H.; Khademhosseini, A. Patterned Differentiation of Individual Embryoid Bodies in Spatially Organized 3D Hybrid Microgels. *Adv. Mater.* **2010**, *22*, 5276−5281.
(21) Lei, Y. F.; Zouani, O. F.; Remy, M. R.; Ayela, C.; Durrieu, M. C. Geometrical Microfeature Cues for Directing Tubulogenesis of Endothelial Cells. *PloS One* **2012**, *7*, e41163.
(22) Lei, Y. F.; Zouani, O. F.; Rami, L.; Chanseau, C.; Durrieu, M. C. Modulation of Lumen Formation by Microgeometrical Bioactive Cues and Migration Mode of Actin Machinery. *Small* **2013**, *9*, 1086−1095.
(23) Xie, J. W.; Liu, W. Y.; MacEwan, M. R.; Yeh, Y. C.; Thomopoulos, S.; Xia, Y. N. Nanofiber Membranes with Controllable Microwells and Structural Cues and Their Use in Forming Cell Microarrays and Neuronal Networks. *Small* **2011**, *7*, 293−297.
(24) Dou, Y. D.; Wu, C. T.; Chang, J. Preparation, Mechanical Property and Cytocompatibility of Poly(L-lacticacid)/calcium Silicate Nanocomposites with Controllable Distribution of Calcium Silicate Nanowires. *Acta Biomater.* **2012**, *8*, 4139−4150.
(25) Dersch, R.; Liu, T.; Schaper, A. K.; Greiner, A.; Wendorff, J. H. Electrospun Nanofibers: Internal Structure and Intrinsic Orientation. *J. Polym. Sci., Part A: Polym. Chem.* **2002**, *41*, 545−553.
(26) Spasova, M.; Mincheva, R.; Paneva, D.; Manolova, N.; Rashkov, I. Perspectives On: Criteria for Complex Evaluation of the Morphology and Alignment of Electrospun Polymer Nanofibers. *J. Bioact. Compat. Polym.* **2006**, *21*, 465−479.
(27) Bordenave, L.; Baquey, C.; Bareille, R.; Lefebvre, F.; Lauroua, C.; Guerin, V.; Rouais, F.; More, N.; Vergnes, C.; Anderson, J. M. Endothelial Cell Compatibility Testing of Three Different Pellethanes. *J. Biomed. Mater. Res.* **1993**, *27*, 1367−1381.
(28) Jaffe, E. A. Culture of Human Endothelial Cells. *Transplant. Proc.* **1980**, *12*, 49−53.
(29) Cornhill, J. F.; Levesque, M. J.; Herderick, E. E.; Nerem, R. M.; Kilman, J. W.; Vasko, J. S. Quantitative Study of the Rabbit Aortic Endothelium using Vascular Casts. *Atherosclerosis* **1980**, *35*, 321−337.
(30) Ives, C. L.; Eskin, S. G.; McIntire, L. V. Mechanical Effects on Endothelial Cell Morphology: in vitro Assessment. *In Vitro Cell. Dev. Biol.: Plant* **1986**, *22*, 500−507.
(31) Sell, S. A.; McClure, M. J.; Garg, K.; Wolfe, P. S.; Bowlin, G. L. Electrospinning of Collagen/biopolymers for Regenerative Medicine and Cardiovascular Tissue Engineering. *Adv. Drug Delivery Rev.* **2009**, *61*, 1007−1019.
(32) Li, Y. H.; Huang, G. Y.; Zhang, X. H.; Wang, L.; Du, Y. N.; Lu, T. J.; Xu, F. Engineering Cell Alignment in vitro. *Biotechnol. Adv.* **2014**, *32*, 347−365.
(33) Li, D.; Wang, Y. L.; Xia, Y. N. Electrospinning Nanofibers as Uniaxially Aligned Arrays and Layer-by-layer Stacked Films. *Adv. Mater.* **2004**, *16*, 361−366.
(34) Wang, B.; Cai, Q.; Zhang, S.; Yang, X.; Deng, X. The Effect of Poly (L-lactic acid) Nanofiber Orientation on Osteogenic Responses of Human Osteoblast-like MG63 Cells. *J. Mech. Behav. Biomed. Mater.* **2011**, *4*, 600−609.
(35) Holzapfel, G. A.; Sommer, G.; Gasser, C. T.; Regitnig, P. Determination of Layer-Specific Mechanical Properties of Human Coronary Arteries with Nonatherosclerotic Intimal Thickening and Related Constitutive Modeling. *Am. J. Physiol.: Heart Circ. Physiol.* **2005**, *289*, H2048−H2058.
(36) Ozolanta, I.; Tetere, G.; Purinya, B.; Kasyanov, V. Changes in the Mechanical Properties, Biochemical Contents and Wall Structure of the Human Coronary Arteries with Age and Sex. *Med. Eng. Phys.* **1998**, *20*, 523−533.
(37) Whited, B. M.; Rylander, M. N. The Influence of Electrospun Scaffold Topography on Endothelial Cell Morphology, Alignment, and Adhesion in Response to Fluid Flow. *Biotechnol. Bioeng.* **2014**, *111*, 184−195.
(38) Sun, T.; Norton, D.; McKean, R. J.; Haycock, J. W.; Ryan, A. J.; MacNeil, S. Development of a 3D Cell Culture System for Investigating Cell Interactions With Electrospun Fibers. *Biotechnol. Bioeng.* **2007**, *97*, 1318−1328.
(39) Zhu, X. L.; Cui, W. G.; Li, X. H.; Jin, Y. Electrospun Fibrous Mats with High Porosity as Potential Scaffolds for Skin Tissue Engineering. *Biomacromolecules* **2008**, *9*, 1795−1801.
(40) Xu, H.; Li, H. Y.; Chang, J. Controlled Drug Release from A Polymer Matrix by Patterned Electrospun Nanofibers with Controllable Hydrophobicity. *J. Mater. Chem. B* **2013**, *1*, 4182−4188.

DOI: 10.1021/acsami.5b00996
ACS Appl. Mater. Interfaces 2015, 7, 8706−8718

(41) Versaevel, M.; Grevesse, T.; Gabriele, S. Spatial Coordination between Cell and Nuclear Shape within Micropatterned Endothelial Cells. *Nat. Commun.* **2012**, *3*, 671−682.
(42) Stiles, J. M.; Pham, R.; Rowntree, R. K.; Amaya, C.; Battiste, J.; Boucheron, L. E.; Mitchell, D. C.; Bryan, B. A. Morphological Restriction of Human Coronary Artery Endothelial Cells Substantially Impacts Global Gene Expression Patterns. *FEBS J.* **2013**, *280*, 4474−4494.
(43) Vaquette, C.; Cooper-White, J. J. Increasing Electrospun Scaffold Pore Size with Tailored Collectors for Improved Cell Penetration. *Acta Biomater.* **2011**, *7*, 2544−2557.
(44) Zhang, D. M.; Chang, J. Patterning of Electrospun Fibers Using Electroconductive Templates. *Adv. Mater.* **2007**, *19*, 3664−3667.
(45) Tseng, P.; Carlo, D. D. Substrates with Patterned Extracellular Matrix and Subcellular Stiffness Gradients Reveal Local Biomechanical Responses. *Adv. Mater.* **2014**, *26*, 1242−1247.
(46) Wise, S. G.; Byrom, M. J.; Waterhouse, A.; Bannon, P. G.; Ng, M. K. C.; Weiss, A. S. A Multilayered Synthetic Human Elastin/Polycaprolactone Hybrid Vascular Graft with Tailored Mechanical Properties. *Acta Biomater.* **2011**, *7*, 295−303.
(47) Dahl, S. L. M.; Rhim, C.; Song, Y. C.; Niklason, L. E. Mechanical Properties and Compositions of Tissue Engineered and Native Arteries. *Ann. Biomed. Eng.* **2007**, *35*, 348−355.

DOI: 10.1021/acsami.5b00996
ACS Appl. Mater. Interfaces 2015, 7, 8706−8718